

Detailed description of exchange bias in CoFe/IrMn

F. Radu, A. W estphalen, K. Theis-B rohl, and H. Zabel

Institut für Experimentalphysik/Festkörperphysik, Ruhr-Universität Bochum, D-44780 Bochum, Germany

(Dated: March 1, 2019)

We show simulations using a modified Maki-Beard model and compare them with longitudinal and transverse hysteresis loops (vector MOKE) from CoFe/IrMn exchange biased bilayers. In the model the interfacial exchange energy is split in two parts, a unidirectional contribution responsible for the exchange bias shift, and an effective uniaxial anisotropy giving rise to the enhanced coercive field observed in all F/AF systems. This is a key feature of the model which we attribute to a spin-glass like behavior of the interface. The simulations are in excellent agreement with the azimuthal dependence of the exchange bias and coercive fields for the complete 360° angular range.

PACS numbers: 75.60.Jk, 75.70.-i, 75.70.Cn

The exchange bias system refers to the shift of the ferromagnetic (F) hysteresis loop to positive or negative values when the F system is in contact with an antiferromagnetic (AF) system and cooled in an applied magnetic field through the Neel temperature of the AF system. The exchange bias phenomenon is associated with the interfacial exchange coupling between ferromagnetic and antiferromagnetic spin structures, resulting in a unidirectional magnetic anisotropy [1]. While the unidirectional anisotropy was successfully introduced by Maki-Beard (M&B), the origin of the enhanced coercive field is yet not well understood. The exchange bias effect is essential for the development of magnetoelectronic switching devices (spin-valves) and for random access magnetic storage units. For these applications a predictable, robust, and tunable exchange bias effect is required.

Extensive data have been collected on the exchange bias field H_{EB} and the coercivity field H_c , for a large number of bilayer systems, which are reviewed in Ref. [2, 3]. The details of the EB effect depend crucially on the AF/F combination chosen and on the structure and thickness of the layers. However, some characteristic features apply to most systems: (1) H_{EB} and H_c increase as the system is cooled in an applied magnetic field below the blocking temperature $T_B = T_N$ of the AF layer, where T_N is the Neel temperature of the AF layer; (2) the magnetization reversal can be different for the ascending and descending part of the hysteresis loop [4, 5, 6, 7], as was first pointed out in reference [8]; (3) thermal relaxation effects of H_{EB} and H_c indicate that a stable magnetic state is reached only at very low temperatures [9, 10, 11]. Several theoretical models have been developed for describing possible mechanisms of the EB effect, including domain formation in the AF layer with domain walls perpendicular to the AF/F interface [13], creation of uncompensated excess AF spins at the interface [14], or the formation of domain walls in the AF layer parallel to the interface [15, 16]. Another approach is the consideration of diluted antiferromagnets in an exchange field. In the work described in Ref. [17, 18, 19] the discussion about compensated versus uncompensated interfacial spins is replaced by a discussion of net magnetic

moments within the antiferromagnetic layer. Depending on the complexity of the system, the models can explain some but not all features of experimental hysteresis loops. Here we report on a EB system for which we can describe all features, including the H_{EB} and H_c dependence on the azimuthal angle.

In the past, less attention has been given to the azimuthal dependence of H_{EB} and H_c . First experiments were performed on NiFe/CoO bilayers [20], where it was suggested that the azimuthal dependence can be best described by a cosine series expansions with odd and even terms for H_{EB} and H_c , respectively. A recent study of IrMn/CoFe bilayers [22] showed that even so good agreement between the data and the simulations based on the cosine functions can be achieved, still some disagreement exists. In an another approach, Mewes et al. [21] showed that the azimuthal dependence of H_c and H_{EB} can be well described within the Stoner-Wohlfarth model. However the magnitude of the coercivity is not explained.

In this paper we report on longitudinal and transverse magnetization curves from CoFe/IrMn exchange bias bilayers. The experimental data have been simulated by a modified M&B model assuming the existence of a spin-glass like interface.

Exchange-biased F/AF bilayers $Ir_{17}Mn_{83}$ (15 nm) = Co₇₀Fe₃₀ (30 nm) were prepared by magnetron sputtering on Si-SiO₂-Cu (30 nm) substrates, covered by a Ta (5 nm) protection layer. The base pressure was below 1×10^{-7} Torr at an Ar pressure of 3×10^{-3} Torr. The initial EB direction is set by an annealing step after deposition for 1 h at 548 K in a magnetic field $H_{ann} = 1$ kOe parallel to the layer plane [23].

The sample was measured using a vector-MOKE setup [24]. A number of 360 pairs of longitudinal and transverse components of the magnetization (m_{jj} and m_{zz} , respectively) were measured for an external field orientation with respect to the field cooling direction ranging from 0 to 360°. All loops were taken at room temperature. In this geometry, the sample is kept fixed during the measurements, whereas the orientation of the applied external field was varied. Characteristic longitudinal and transverse magnetization curves are shown in Fig. 1. In

order to observe the modulations of the EB field, the one degree step variation of the azimuthal angle is required. The hysteresis loops provide the coercive fields H_{c1} and H_{c2} as shown in Fig. 2a which further provides the coercive field $H_c = (H_{c1} + H_{c2})/2$ and the EB field $H_{EB} = (H_{c1} + H_{c2})/2$ as plotted in Fig. 3a.

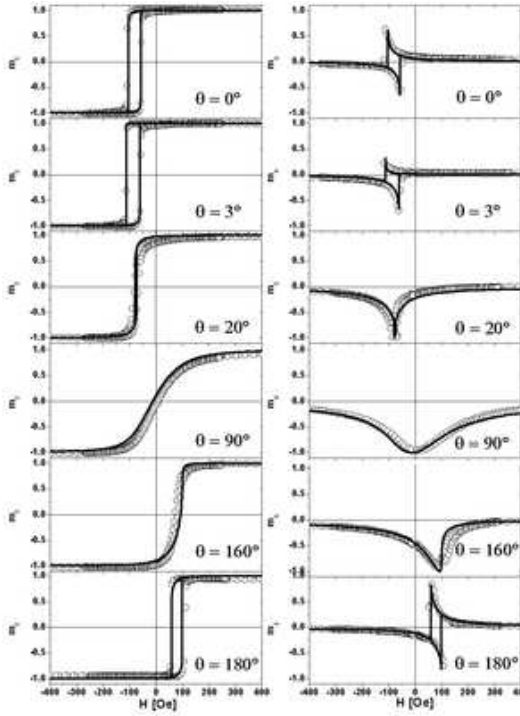


FIG. 1: Experimental (open circles) and simulated hysteresis loops (black lines) for different azimuthal angles. The simulated curves are calculated by the Eq. 3 with the following parameters: $f = 80\%$; $R = 5.9 = f$; $\gamma = 20$.

We first discuss the experimental observations in Figs. 1, 2a, and 3a. In Fig. 1 some representative longitudinal and transverse loops are shown. A distinct feature of the system is that the magnetization reversal occurs via coherent rotation as seen from the non-vanishing transverse loops, which are completely reproduced by numerical simulations (solid lines), to be discussed further below. The maximum exchange bias field is $H_{EB} = 90$ Oe and it is achieved at $\theta = 20^\circ$ (see Fig. 3), where θ is the azimuthal angle with respect to the field cooling direction defined as $\theta = 0$. This is one of the salient features reported here, as usually the maximum of the EB field is believed to occur parallel to the field cooling direction.

The longitudinal hysteresis loop at $\theta = 0$ is completely symmetric. This is also seen in the transverse magnetization, where the forward and reverse components have the same magnitude, but are doubly mirrored with respect to $\theta = 0$ and H_{EB} . This is not always the case. For instance, only a few degrees forward at $\theta = 3^\circ$ both, longitudinal and transverse loops become asymmetric. The forward branch of the hysteresis loop is steep, while the

reverse branch is more rounded. It is remarkable that within an azimuthal angle of only 3° such a strong asymmetry of the hysteresis loop develops. This asymmetry is different from the one observed due to the training effect [4, 7]. The former is completely reversible while the latter is not.

As the azimuthal angle is further increased, H_c disappears at about $\theta = 20^\circ$ and reappears again, in a symmetric manner, close to 160° . The vanishing coercive field can be understood from the transverse loops, where it is clearly seen that the rotation of the ferromagnetic spins do not make a complete 360° rotation, but almost reversibly rotate within the half circle of 180° . Therefore the angle of the magnetization orientation, from which the coercive fields are extracted, takes the same value for both H_{c1} and H_{c2} .

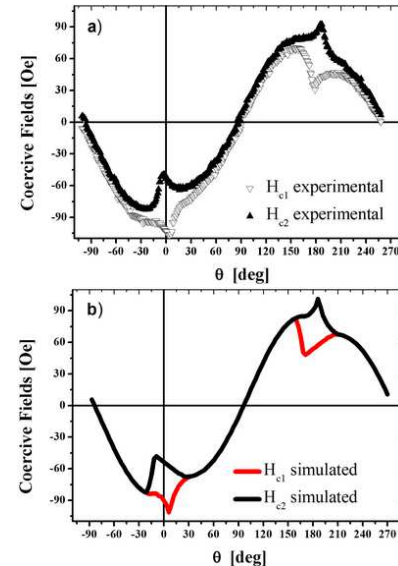


FIG. 2: a) Azimuthal dependence of the coercive fields H_{c1} (filled symbol) and H_{c2} (open symbols) extracted from the experimental hysteresis loops. At $\theta = 0; 180^\circ$, which corresponds to the field cooling direction the coercive fields deviate one from each other within a 20° angular range. b) Calculated coercive fields H_{c1} and H_{c2} as a function of the azimuthal angle, using Eq. 3 with the following parameters: $f = 80\%$; $R = 5.9 = f$; $\gamma = 20$.

In Fig. 2a the coercive fields are plotted versus the azimuthal angle θ . We notice that, globally, they follow the expected unidirectional behavior [1], but some striking deviations are recognizable. In particular, close to the field cooling direction spike like features appear. While the coercive fields H_{c1} and H_{c2} are well behaved for most of the angles, this is not the case for field directions close to the field cooling orientation. Here H_{c1} and H_{c2} deviate one from each other, resulting in a non-vanishing coercive field as seen in Fig. 3a. Its maximum value ($H_{c1}^{MAX} = 20$ Oe) is about four times lower than the maximum value of the exchange bias field. Finite values are observed within a 20° degree range centered

at $\theta = 0$ and $\theta = 180$ and almost vanish outside this range.

The H_{EB} dependence on the azimuthal angle (solid symbols in Fig. 3a) clearly shows the unidirectional anisotropy. In addition a peculiar and sharp modulation is seen with a low amplitude. These features appear close to the cold cooling orientation and also close to the opposite orientation. They cannot be reproduced satisfactorily with the empirical description based on a cosine series expansion as suggested in Ref. [20]. Therefore we need a more realistic model, which is discussed next.

The M & B model [1] assumes that the AF spins rigidly form an AF state, but they may slightly rotate as a whole during the magnetization reversal of the F layer. Within the M & B model, enhanced coercivity is not accounted for. The interface is assumed to be perfectly uncompensated with the interface AF spins having the same anisotropy as the bulk spins. However, the interface is never perfect. Roughness, deviations from stoichiometry, interdiffusion, structural defects, etc. cause non-ideal magnetic interfaces. It is therefore naturally to assume that, statistically, a fraction of the AF spins have lower anisotropy as compared to the bulk ones. These interfacial AF spins can rotate together with the ferromagnet. They mediate the exchange coupling, induce an enhanced coercivity, but soften the extreme coupling condition assumed by M & B. Therefore, we assume that the anisotropy of the AF interface layer varies from $K_{int} = 0$ next to the F layer to $K_{int} = K_{AF}$ next to the AF layer, where K_{AF} is the anisotropy constant of a presumably uniaxial antiferromagnet. This variation of the anisotropy constant across the interface governs the enhanced anisotropy of the ferromagnetic layer. So far it was believed that the enhanced coercivity in F/AF exchange biased systems is caused by compensated AF spins at the F/AF interface. We argue that for most of the AF materials a compensated or uncompensated spin having the same anisotropy as the bulk AF layer would be practically impossible to reverse by rotating the F layer. Therefore we need to assume low anisotropy AF spins in order to quantitatively describe the experimental data.

A direct indication of the rotating AF spins is revealed by soft X-ray magnetic dichroism [25, 26]. Element specific hysteresis loops show that some spins belonging to the AF layer rotate reversibly with the F spins. Due to the shift of the hysteresis loop it is obvious that another part of the AF layer is frozen. Therefore the AF layer can be considered, to a first approximation, as consisting of two types of AF states. One part having a large anisotropy preserving the AF state and another interfacial part with a weaker anisotropy, allowing the spins to rotate together with the F spins. Moreover, polarized neutron scattering [4, 7] revealed two further effects related to the magnetic state of the CoO/Co interface (which is similar to the CoFe/IrMn system [27]) during the magnetization reversal: a) the interface is disordered containing domains and domain walls even in saturation, similar to a spin-glass (SG) system; b) the interfacial fer-

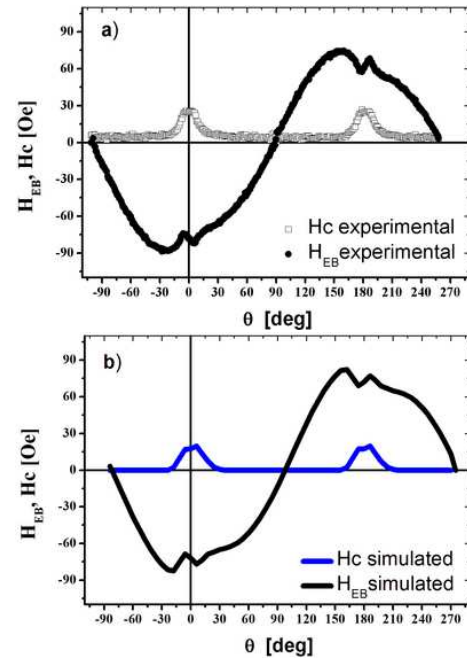


FIG. 3: a) The experimental coercive field and exchange bias field as a function of the azimuthal angle. The cold cooling orientation corresponds to $\theta = 0$. b) Simulated coercive field and exchange bias field as a function of the azimuthal angle. The curves are delivered by the Eq. 3 with the following parameters: $f = 80\%$; $R = 5.9 = f$; $\alpha = 20$

romagnetic spins are not collinear with the applied field direction during the reversal.

The experimental results mentioned above are in our model accounted for by two averaging interface properties: (a) the existence of low AF anisotropy spins, to which we assign an effective average anisotropy K_{SG}^{eff} ; (b) a non-collinearity angle α . Adding these two parameters, the modified M & B model reads:

$$\begin{aligned} E = & -J_{0H} M_F t_F \cos(\theta) + K_F t_F \sin^2(\theta) \\ & -J_{0H} M_{SG} t_{SG} \cos(\theta) + K_{SG}^{eff} \sin^2(\theta) \\ & + K_{AF} t_{AF} \sin^2(\theta) \\ & - J_{eb}^{eff} \cos(\theta); \end{aligned} \quad (1)$$

where J_{eb}^{eff} is the reduced interfacial exchange energy, and the angle is the average angle of the effective SG anisotropy, M_{AF} is the magnetization of the SG interface, and t_{SG} is the SG interface thickness. For simplifying the numerical analysis we neglect the $J_{0H} M_{SG} t_{SG}$ term, because $M_{SG} t_{SG}$ is very small. Furthermore we neglect the crystal anisotropy of the ferromagnetic layer ($K_F = 0$) as it does not contribute essentially to the properties of the EB system.

The interface anisotropy, which leads to enhanced coercivity, characterizes the quality of the interface. When K_{SG}^{eff} is zero, the system behaves ideally as described by the M & B model [1], i.e. the coercive field is zero and the

exchange bias field is finite. In the other case when the interface is disordered, we relate the effective SG anisotropy to the available interfacial coupling energy as follows:

$$\begin{aligned} K_{\text{eff}} &= (1-f) J_{\text{eb}} \\ J_{\text{eb}}^{\text{eff}} &= f J_{\text{eb}}; \end{aligned} \quad (2)$$

where J_{eb} is the total exchange energy of an ideal system, which shows no additional coercivity. With this assumption the absolute value of the exchange bias field is reduced as compared with the M & B model by the factor f . The factor f describes the conversion of interfacial energy into coercivity.

Next, we write the system of equations resulting from the minimization of the Eq. 1 with respect to the and angles:

$$\begin{aligned} h \sin(\theta) + (1-f) \sin(2\phi) + f \sin(\phi) &= 0 \\ R \sin(2\phi) - f \sin(\phi) &= 0; \end{aligned} \quad (3)$$

where, $h = H = [J_{\text{eb}}^{\text{eff}} = (M_F t_F)]$ is the reduced field, and $R = K_{\text{AF}} = (t_{\text{AF}} J_{\text{eb}}^{\text{eff}})$ is the R-ratio defining the strength of the AF layer. This system of equations can easily be solved numerically, but it cannot deliver a simple analytical expression for the exchange bias. Numerical evaluation provides the angles and as a function of the applied magnetic field H . The reduced longitudinal and transverse components of the magnetization are $m_{\parallel} = \cos(\phi)$ and $m_{\perp} = \sin(\phi)$, respectively. These are the two observables measured by vector-M OKE. Note that the anisotropic magnetoresistance (AMR) and PNR hide the chirality of the ferromagnetic spin rotation as they provide $\sin^2(\phi)$ information, whereas M OKE reveals the chirality as it provides $\sin(\phi)$ information.

In Fig. 1 calculated magnetization components are plotted together with the experimental data points, and

in Figs. 2b and 3b the azimuthal dependence of the coercive fields and exchange bias field are plotted and compared to the experimental data in Fig. 2a and 3a. In all cases the calculated curves are in excellent agreement with the experimental data. It is remarkable, that the azimuthal dependence of the exchange bias field and the coercive fields (H_{c1}, H_{c2}, H_c) observed experimentally, are completely reproduced by the SG model. The parameters used are: $f = 20\%$, $R = 20$ and $R = 5.9 = f$. For calculating the value of the R-ratio we used the anisotropy constant (K_{AF}) measured in Ref. [28]. The conversion factor is related to the magnitude of the coercive field with respect to the shift of the loop. The angle plays an important role. For instance, when is zero, the coercive field is much enhanced at $\phi = 0; 180^\circ$ as compared to the experimental data, and the azimuthal dependence of H_{EB} and H_c cannot be reproduced.

In conclusion, we have measured the longitudinal and transverse components of the magnetization vector for an exchange biased CoFe/FeMn system. From the experimental data we extracted the azimuthal dependence of the exchange bias and the coercive field. The azimuthal dependence of the exchange bias effect was successfully simulated via a modified Meiklejohn and Bean type model, taking into account a realistic state of the interface, which induces enhanced coercivity in the ferromagnetic layer. A striking agreement between calculations and experiments was achieved using a spin glass like model.

We would like to thank J. Schmalhorst, V. Hoink, and H. Brückl from the University of Bielefeld for providing the samples. We gratefully acknowledge support through the Sonderforschungsbereiche 491 "Magnetische Heteroschichten: Struktur und elektronischer Transport" of the Deutsche Forschungsgemeinschaft.

[1] W. H. Meiklejohn and C. P. Bean, *Phys. Rev.* **102**, 1413 (1956); *Phys. Rev.* **105**, 904 (1957).
[2] A. E. Berkowitz, K. Takano, *J. Magn. Magn. Mater.*, **200**, 552-570 (1999).
[3] J. Nogues, I. K. Schuller, *J. Magn. Magn. Mater.*, **192**, 203-232 (1999).
[4] F. Radu, et al., *J. Magn. Magn. Mater.*, **240**, 251 (2002).
[5] M. Gierlings, et al., *Phys. Rev. B* **65**, 092407 (2002).
[6] W.-T. Lee, et al., *Phys. Rev. B* **65**, 224417 (2002).
[7] F. Radu, et al., *Phys. Rev. B* **67**, 134409 (2003).
[8] M. R. Fitzsimmons, et al., *Phys. Rev. Lett.* **84**, 3986 (2000).
[9] D. S. Gogeghegan, P. G. McCormick, R. Street, *J. Magn. Magn. Mater.* **177**, 937 (1998).
[10] A. M. Goodman, et al., *J. Appl. Phys.* **87**, 6409 (2000).
[11] F. Radu, et al., *Appl. Phys. A* **74** Suppl., S1570 (2002).
[12] J. Nogues, et al., *Phys. Rev. Lett.* **76**, 4624 (1996).
[13] A. P. Malozemoff, *Phys. Rev. B* **35**, 3679 (1987).
[14] T. C. Schulthess and W. H. Butler, *Phys. Rev. Lett.* **81**, 4516 (1998).
[15] D. Mauri, et al., *Appl. Phys.*, **62**, 3047 (1987).
[16] Joo-Von Kim and R. L. Stamps, *Phys. Rev. B* **71**, 094405 (2005).
[17] P. Miltz, et al., *Phys. Rev. Lett.* **84**, 4224 (2000).
[18] J. Keller, et al., *Phys. Rev. B* **66**, 014431 (2002).
[19] U. Nowak, et al., *Phys. Rev. B* **66**, 014430 (2002).
[20] T. Ambrone, et al., *Phys. Rev. B* **56**, 83 (1997).
[21] T. Mewes, et al., *Phys. Rev. B* **65**, 224423 (2002).
[22] L. E. Fernandez-Oloton, K. O'Gallagher, *J. Magn. Magn. Mater.* **290-291**, 536 (2005).
[23] V. Hoink, et al., *Appl. Phys. Lett.* **86**, 152102 (2005).
[24] A. Westphalen, et al., to be published (2005).
[25] H. Ohldag, et al., *Phys. Rev. Lett.* **91**, 017203 (2003).
[26] F. Radu, et al., to be published, (2005).
[27] J. M. Good, et al., *J. Appl. Phys.* **93**, 5491 (2003).
[28] K. Steenbeck, et al., R. M. Attheis and M. Diegel, *J. Magn. Magn. Mater.* **279**, 317 (2005).